Supporting Information for

Improved anaerobic degradation of purified terephthalic acid wastewater by adding nanoparticles or co-substrates to facilitate the electron transfer process

Heng Li[a,b], Weidong Zhang[a], Dong Xia[a], Lingfen Ye[a], Wende Ma[a], Haiyan Li[b], Qingbiao Li[c], Yuanpeng Wang[a]*

Experimental Methods

The composition of artificial wastewater (per litre):

Carbon source; NH_4Cl, 0.956 g; $Na_2HPO_4 \cdot 12H_2O$, 0.252 g; KH_2PO_4, 0.11 g; $CaCl_2$, 0.18 g; Trace element I, 1 mL; and trace element II, 1 mL. The pH was adjusted to approximately 7.2 ± 0.1 through adding $NaHCO_3$. The composition of trace elements (in grams per litre) was as follows: trace element I: EDTA, 5000; $FeSO_4$, 5000. Trace element II: EDTA, 15000; $NaMoO_4 \cdot 2H_2O$, 220; $CoCl_2 \cdot 6H_2O$, 240; $NiCl_2 \cdot 6H_2O$, 190; $ZnSO_4 \cdot 7H_2O$, 430; H_3BO_4, 14; $MnCl_2 \cdot 4H_2O$, 990; $CuSO_4 \cdot 5H_2O$, 250.

The detailed operations of the seven reactors:

R_2 and R_3 were added with 5 g/L TiO_2 NPs and 5 g/L Fe_3O_4 NPs respectively, and were well mixed with the activated sludge. The running time of 220 days in R_4 (ethanol-added) was divided into three stages (I, II and III). In stage I (0-39 days), the carbon source of the three reactors was benzoic acid (BA). The influent TOC was gradually increased from 1300 mg/L to 1500 mg/L and finally maintained at 1800 mg/L, aiming to impart the reactor system with degradation capabilities of aromatic compounds. After 39 days of operation, in stage II (40-79 days), the carbon source of the three reactors was changed to a mixture of BA and TA, for training the TA degradation capabilities of the entire system. Their proportions gradually decreased from 4:1 to 3:2 (in a ratio of TOC). After 79 days of cultivation, ethanol as a co-substrate was added in (80-220 days). On day 80, equivalent ethanol was added to replace the BA as co-substrates, and continuously operated till day 220 (stage III). In R_5, R_6 and R_7, the IPA concentrations increased stepwise in an order of 1800, 3000, 6000, 15000 and 18000 mg/L in the three

reactors. In the stage I (0-133 days) and stage II (134-161 days), the carbon source of the three reactors were BA and IPA, with a TOC ratio of 1:2 and 1:3, respectively. In the stage III (162-181 days), stage IV (182-213 days) and stage V (214-252 days), IPA was used as the only carbon source, the influent IPA was increased from 6000 mg/L (stage III) to 15000/mg L (stage IV), and finally stay at 18000 mg/L (stage V). Throughout the experimental process, hydraulic retention time (HRT) was all set to 9 h and pH was kept at 7.2. Meanwhile, the production of gas, content of methane and changes of TOC values were monitored every two days. At the end of experiment, the conductivity of the granular sludge and the microbial community of each reactor were determined.

The determination of optimal nanomaterials concentrations:

The optimal usage amount of TiO_2 nanoparticles was predetermined by batch experiments, and the results regarding TA degradation performances of 1, 2.5, 5 and 10 g/L are shown in below Figure S1. As observed, the TA degradation rates were gradually increasing with the increase of nanoparticle amount, but showing no obvious variations at 5 g/L and 10 g/L. While the most commonly utilized amount of Fe_3O_4 is in the range of 4.6 - 10 g/L,[1-3] considering an accurate comparison of the two nanoparticles in affecting degrading performances, therefore both usage amount of TiO_2 and Fe_3O_4 nanoparticles in this study were adopted 5 g/L.

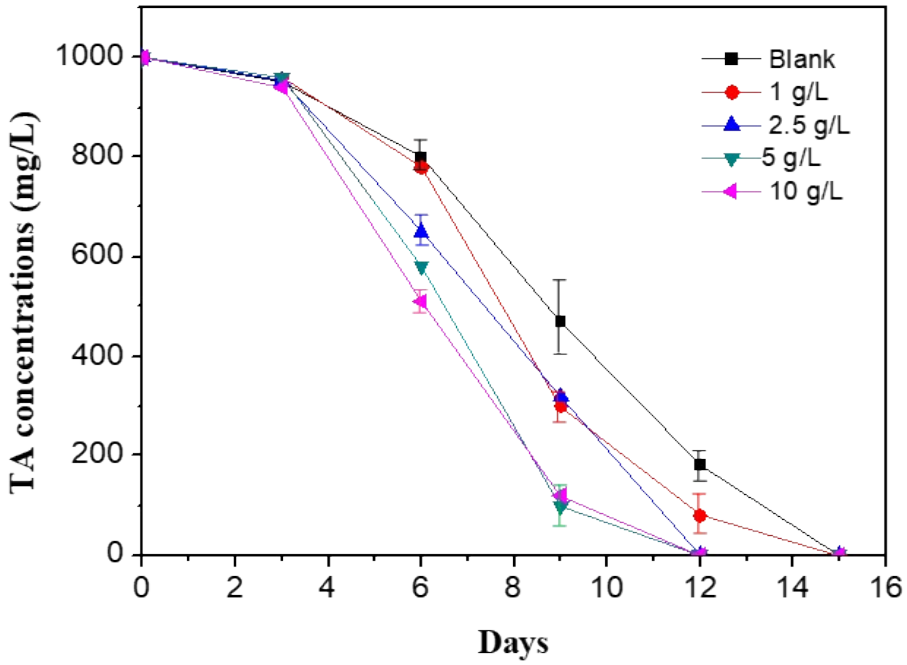

Figure S1. Effect of different mass of TiO_2 nanomaterials on TA degradation.

The solid phase extraction:

The dehydrated extracts were concentrated by a rotary evaporator at 40 ^{o}C, followed by redissolving in ethyl acetate. Then, 0.1 mL N,O-bis(trimethylsilyl)acetamide was added into the obtained organic solution and was left for 30 min at 60 ^{o}C. The derivatized samples were then transferred to an autosampler vial for GC/MS analysis. The oven temperature was initially maintained at 60 ^{o}C for 1 min, programmed to 200 ^{o}C at 5 ^{o}C min^{-1} (hold 5 min) and then increased to 280 ^{o} C at 15 ^{o}C min^{-1} (hold 5 min) at last. The transfer line and ion source temperatures were 250 ^{o}C and 200 ^{o}C, respectively, and the electron energy was 70 eV.

Pyrosequence data analysis:

On the basis of sequence barcodes, trimming and assignment work were done to each sample for all sequence reads. For downriver analysis, the high qualified sequence (average base quality score >30 and length >300bp, without ambiguous base 'N') will be chosen. With a 97% identity threshold, the sequences were then clustered into operational taxonomic units (OTUs). The aligned gene sequences were analyzed for chimera checking in 16s rDNA method with the Uchime algorithm.[4] All of the samples were randomly resampled to 17620 reads. We made Shannon's diversity index and beta-diversity (PCA, UniFrac) analyses, for which the rarefaction curves were generated from the observed species. Taxonomy was assigned using the Ribosomal Database Project classifier.[5] Taxonomy was assigned using silva128/16s database.

Additional discussion

The TA degradation in the R_1, R_2 and R_3 reactor during the 0-157 days:

During the 0-100 days, there was almost no degradation sign of TA in the R_1, R_2 and R_3 reactor (Figure 2a-2c), and the three reactors continued to display relatively low degradation performance without significant difference during the next following 101-130 days. After 130 days, the TA degradation rates of the three reactors showed an obvious trend of fast growth.

The change of the dominant microbes in the four reactors at phylum level

After adding nanoparticles, the relative abundance of *Proteobacteria* and *Euryarchaeota* changed significantly, the *Euryarchaeota* in R_2 (25.4%) and R_3 (25.0%) were increased by 15.1% and 7.9%, compared to R_1 (14.3%). While the *Proteobacteria* in R_2 (20.4%) and R_3 (18.1%) decreased by 19.7% and 9.3%, compared to R_1 (28.5%). The same variation trend was also found in R_4, with the relative abundance of *Euryarchaeota* reaching up to 58.7%.

The reasons for starting the reactors of R_5, R_6 and R_7:

The TiO_2 NPs and Fe_3O_4 NPs present clearly different physicochemical properties, but the two showed no significant discrepancies in terms of promoting the degradation of TA (1000 mg/L). Evidently, Fe_3O_4 NPs displayed considerably higher promotion effects in degrading high-concentration TA wastewater (7000 mg/L) than the batch experiments using TiO_2 NPs (Figure S2). Unfortunately, the influent water with the simulated TA concentration over 3000 mg/L will cause blockage in the UASB system due to the low solubility of TA. In order to fully understand whether nanoparticles can promote degrading other components in the PTA wastewater while still use the UASB system, as well as whether they will exhibit clear discrepancies in dealing with high-concentration pollutants, therefore three new reactors were designed to degrade high-concentration IPA wastewater (will not cause blockage under high-concentration in the UASB system), by using the nanoparticle-free reactor R_5, the TiO_2-added reactor R_6 and the Fe_3O_4-added reactor R_7.

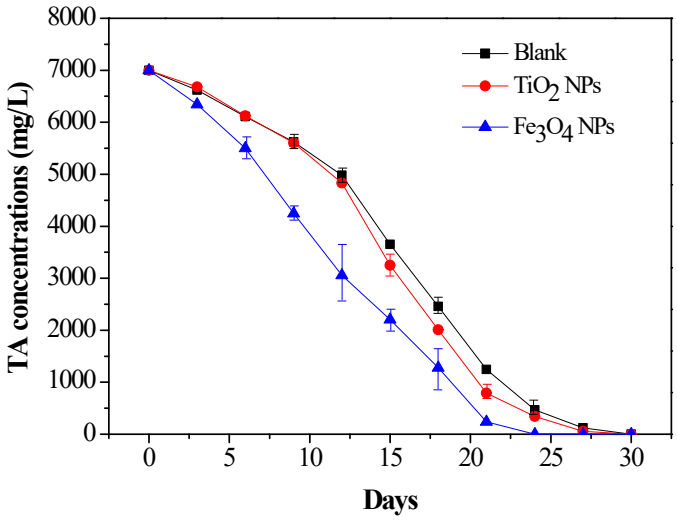

Figure S2. Degradation performances of TA (7000 mg/L) wastewater in blank reactor, TiO_2-added reactor and Fe_3O_4-added reactor.

IPA degradation in R_5, R_6 and R_7 in the first three stages

The obvious degradation of IPA started on day 66 (Figure 7a), and then the degradation rate reached up to 100% in the later stage of phase I (day 95). In phase II (134-161 days), the concentration of IPA was increased from original 1800 to 3000 mg/L, which profiled no sign of affecting degradation rates in all the three reactors, i.e. they were steadily maintained at 100%. Notably, in phase III (134-161 days), the concentration of IPA was further increased up to 6000 mg/L (during this stage, the BA in phase I and phase II has been completely replaced by IPA), but the degradation rate of IPA reached up to 100% again and was remained stable after a brief decline in all three reactors, confirming that the degradation of high concentration IPA by adding nanoparticles was of high efficiencies.

The possible reason for the higher performance with Fe_3O_4 to degrade high-concentration IPA：

For low-concentration TA wastewater, TiO_2 nanoparticles as semi-conducting materials show electric-conducting properties that enable to promote DIET process, therefore displaying similar promotion effects that are analogous with highly conducting Fe_3O_4 nanoparticles. Similar studies have also been reported, for example Chen et al. found that the addition of biochar promoted the DIET process between Geobacter metallireducen and Methanosarcina barkeri, and the promotion effects were similar to granular activated carbon, but the conductivity of biochar was only 1/1000 of that granular activated carbon.[6] As to the high-concentration IPA wastewater, the electron transfer efficiencies in degrading high loads of organic compounds play essential roles, therefore the highly-conducting Fe_3O_4 nanoparticles showed significantly enhanced DIET performances owing to high conductivity. As proved by Lei et al.,[7] in coping reactors with high organic loads (e.g. up to 18.2 kg/COD/m^3/d), the Fe_3O_4 nanoparticles-added reactors presented particularly high promotion effects compared to reactors with relatively low organic loads. Consequently, the semiconducting properties of TiO_2 nanoparticles are unavailable to provide enough free electrons in remedying high-concentration PTA wastewaters, while the highly conductive Fe_3O_4 nanoparticles reach the requirements that are highly consistent with previously reported studies.[3]

The economic analysis of nanoparticles addition:

The prices for TiO_2 and Fe_3O_4 were about 22 \$/kg and 25 \$/kg, respectively. As the addition amount of nanoparticle was 5 g/L when only the reactor was started, therefore the costs for our UASB reactors (4.3 L) were corresponding 0.47 \$ and 0.54 \$, and no extra addition was required during the rest operation, i.e. no extra costs will be generated, therefore, adding nanoparticles into UASB reactors are inexpensive and convenient. Additionally, the operation of our UASB reactor required about 1 kw·h of electricity per day, while the addition of nanoparticles shortened 50 days of complete TA degradation, therefore saving 50 kw·h of electricity, namely saving 3.92 \$. Consequently, the addition of TiO_2 and Fe_3O_4 nanoparticles into UASB reactor for degrading large-volume PTA wastewater is a cost-effective approach.

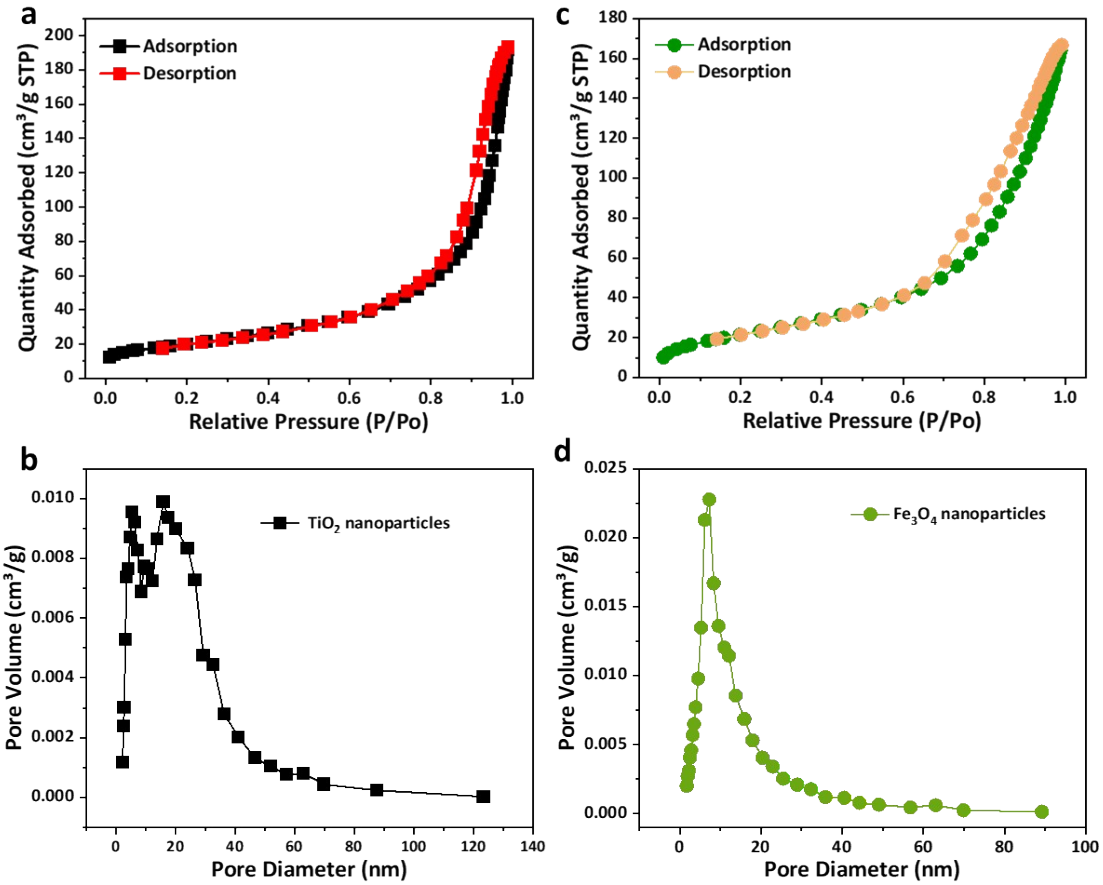

Figure S3. Nitrogen adsorption/desorption curves of TiO_2 nanoparticles (a) and Fe_3O_4 nanoparticles (c). Pore size distribution of TiO_2 nanoparticles (b) and Fe_3O_4 nanoparticles (d).

BET surface areas of TiO_2 nanoparticles and Fe_3O_4 nanoparticles were 71.7 m^2/g and

80.4 m^2/g, respectively. Both the nitrogen adsorption/desorption curves indicated typical type-IV loops (Figure S3a and Figure S3c), demonstrating the ample existence of mesopores. Nevertheless, the two nanoparticles presented clearly different mesopore distributions, with the size manly centering at 15.9 nm for TiO_2 nanoparticles (Figure S3b) and 7.1 nm for Fe_3O_4 nanoparticles (Figure S3d).

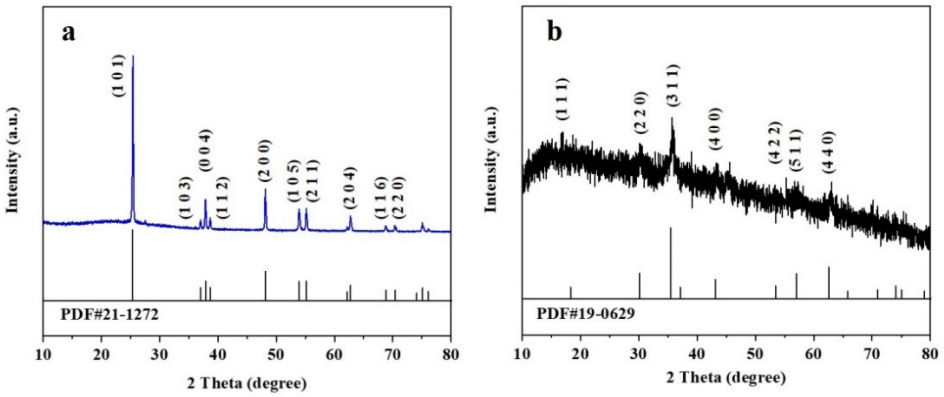

Figure S4. XRD patterns of TiO_2 nanoparticles (a) and Fe_3O_4 nanoparticles (b).

The crystal phases of TiO_2 and Fe_3O_4 nanoparticles were confirmed by XRD patterns, as shown in Figure S4. For the TiO_2 nanoparticles, various characterization peaks emerged (Figure S4a), belonging to (101), (103), (004), (112), (200), (105), (211), (204), (116), and (220) crystal planes. While the characterization peaks in Fe_3O_4 nanoparticles were assigned to (111), (220), (311), (400), (422), (511) and (440) crystal planes (Figure S4b).

The surface morphology was characterized by SEM technique (as observed in Figure S5), and the micrographs indicated that both the TiO_2 and Fe_3O_4 nanoparticles showcased irregular spheres with sizes below 100 nm, corroborating their nanoscale characters.

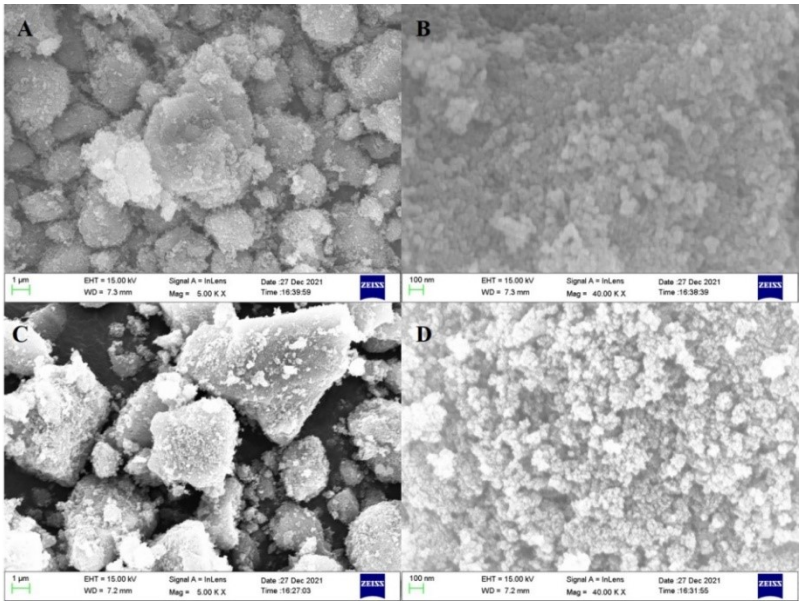

Figure S5. SEM images of TiO_2 nanoparticles (A, B) and Fe_3O_4 nanoparticles (C, D).

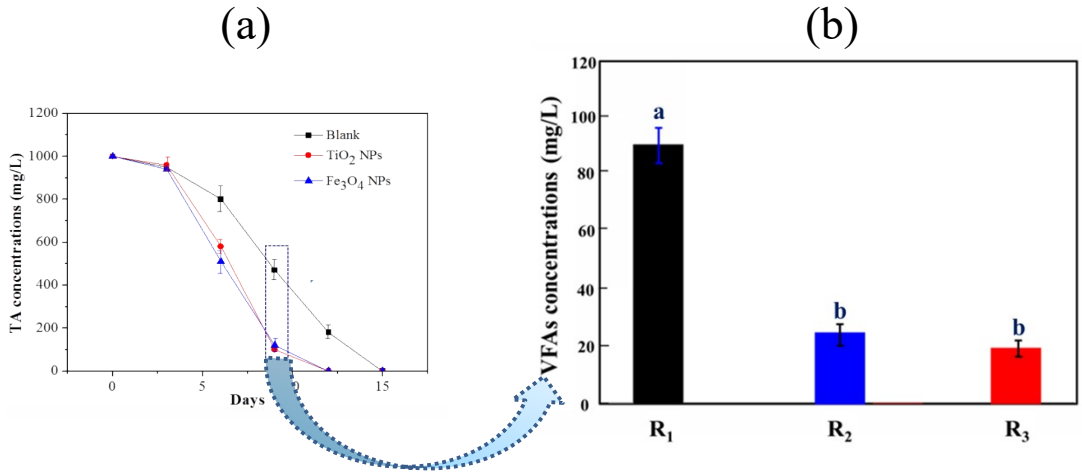

Figure S6. Degradation of TA (1000 mg/L) in blank, TiO_2-added and Fe_3O_4-added reactors (a). VFAs concentrations during TA degradation in blank (R_1), TiO_2-added (R_2) and Fe_3O_4-added (R_3) reactors (b). Data of the different reactors marked with different case letters were significantly different at $p < 0.05$.

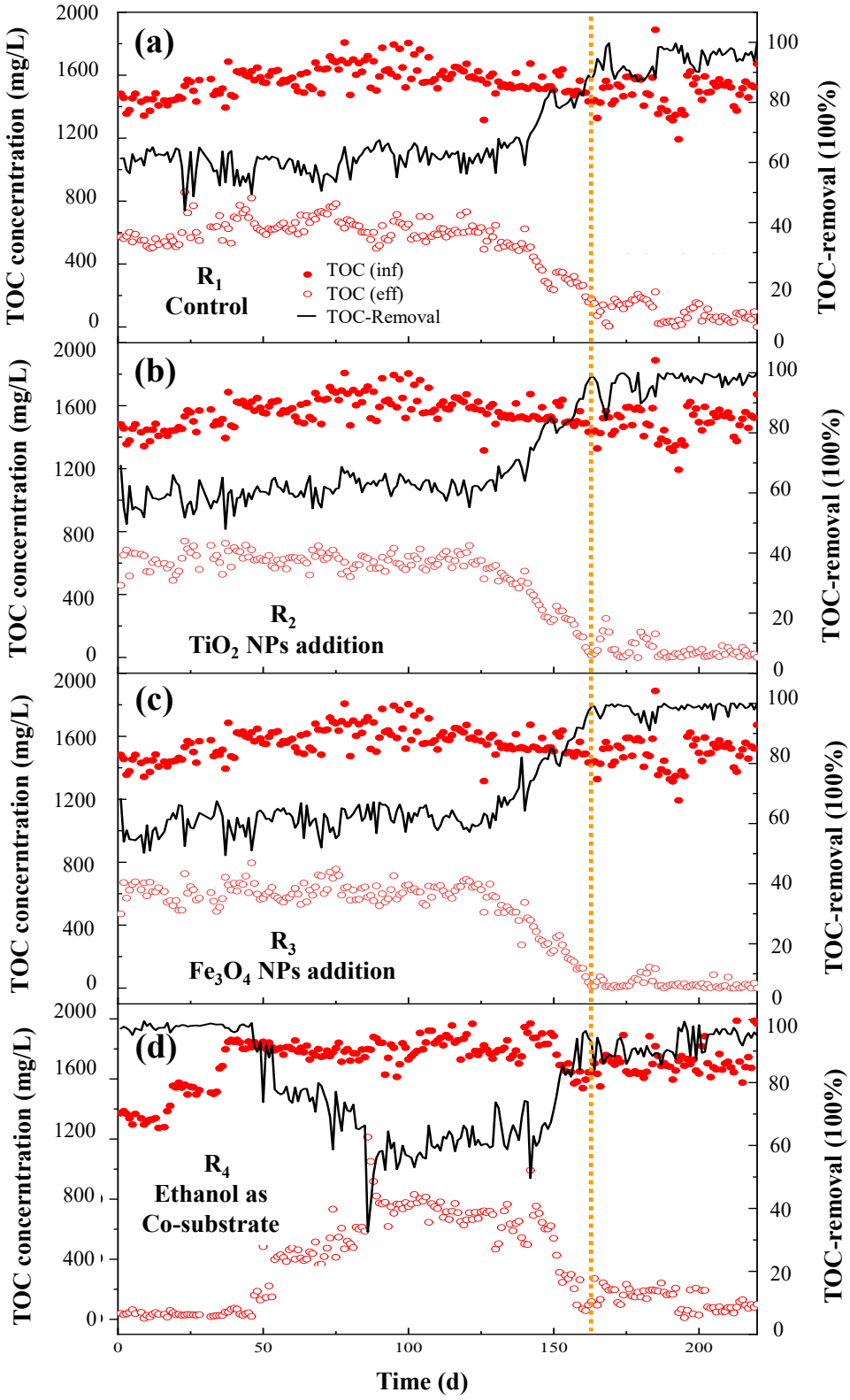

Figure S7. Degradation rates of TOC in R_1 (a), R_2 (b), R_3 (c) and R_4 (d) as a function of operating days (TOC: total organic carbon).

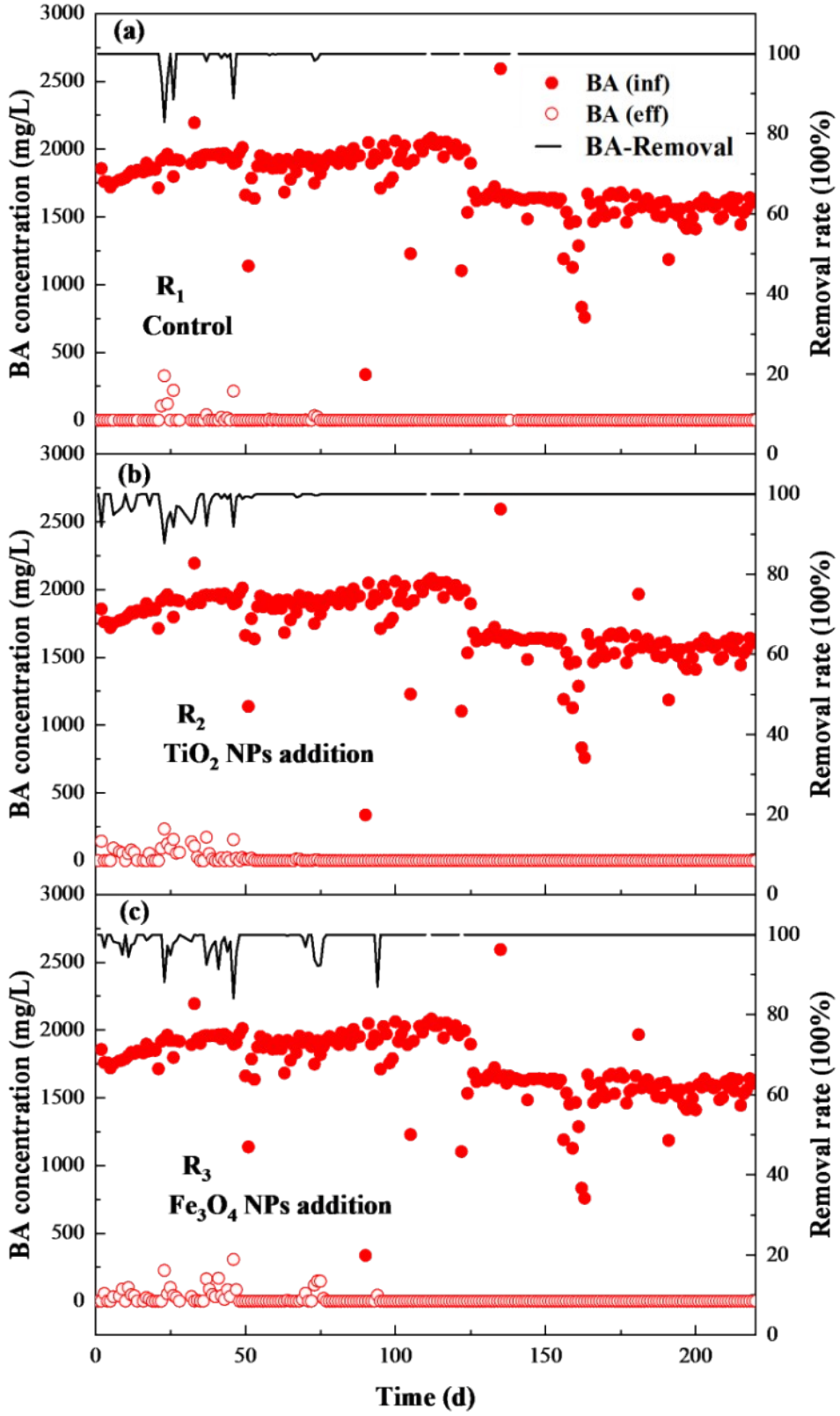

Figure S8. The degradation rate of BA in R_1 (a), R_2 (b), R_3 (c) and R_4 (d) as a function of operating days.

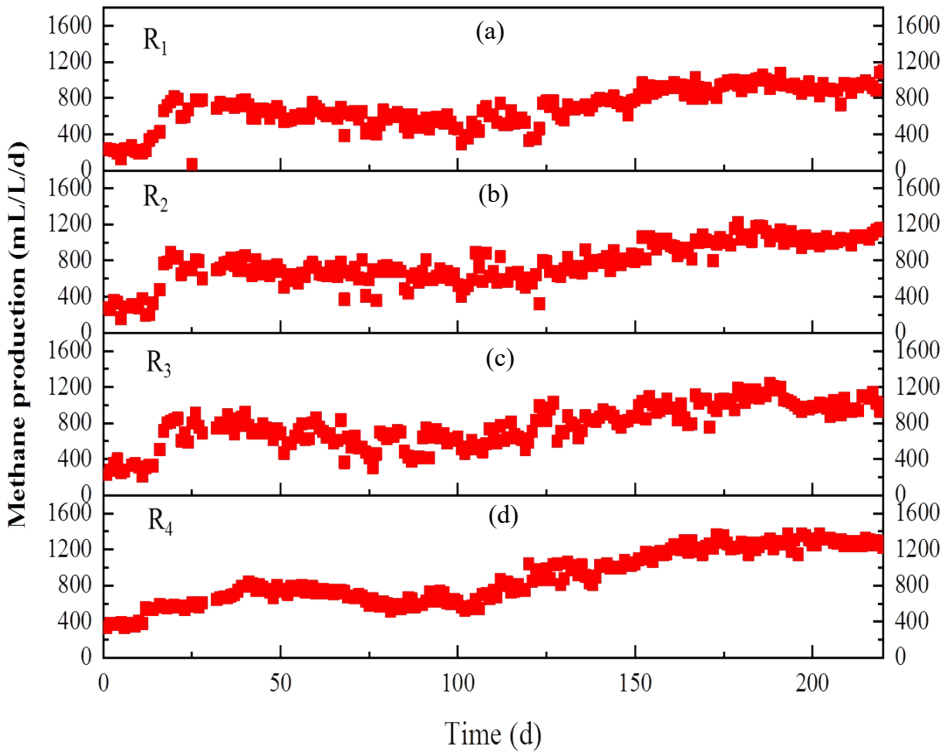

Figure S9. Methane production in R_1 (a), R_2 (b), R_3 (c) and R_4 (d) as a function of operating days.

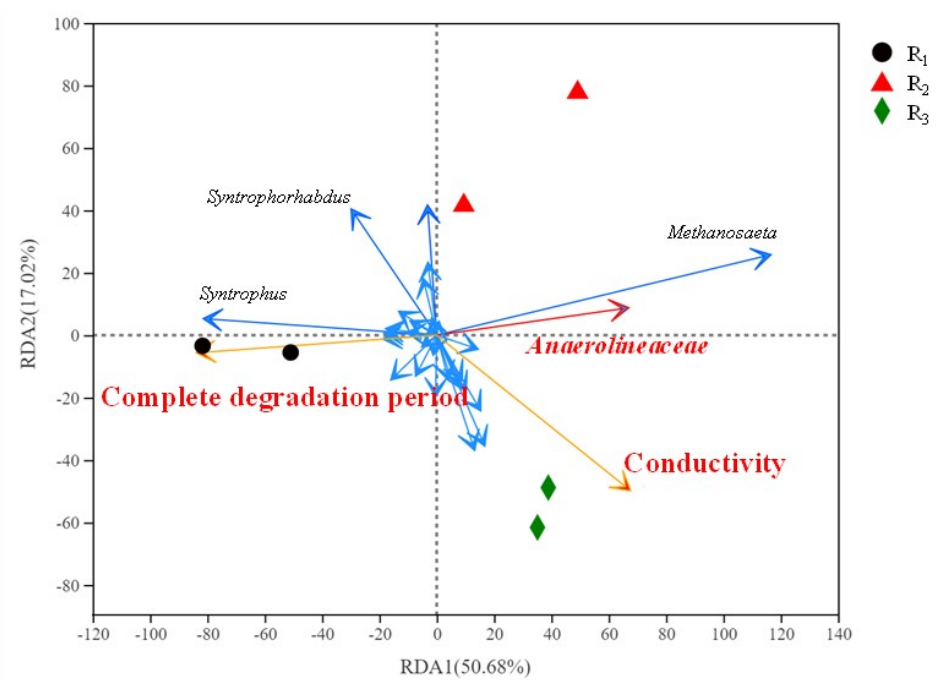

Figure S10. Redundancy analysis (RDA) between the granular sludge conductivity and the complete TA degradation period in R_1, R_2 and R_3.

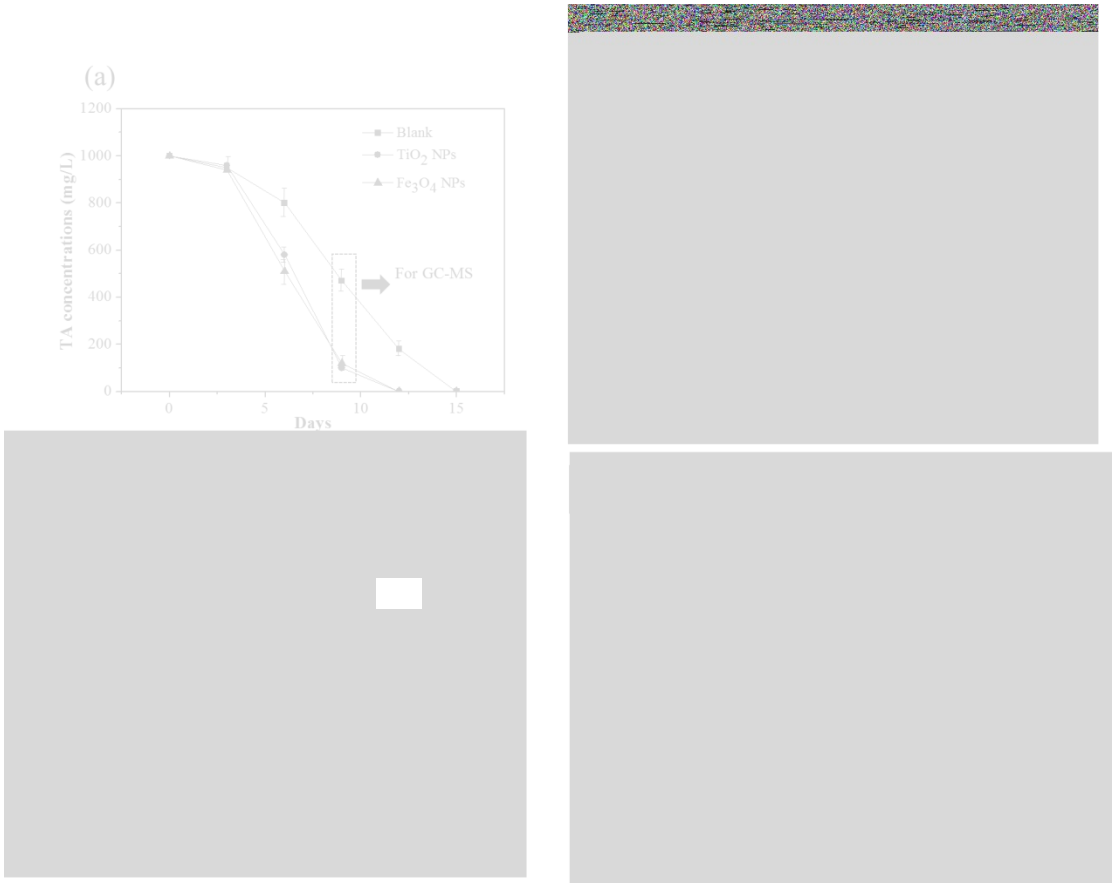

Figure S11. Degradation of TA (1000 mg/L) in blank, TiO_2-added and Fe_3O_4-added reactors (a). GC/MS analysis of intermediates during TA degradation from the blank reactor (b), TiO_2-added reactor (c) and Fe_3O_4-added reactor (d).

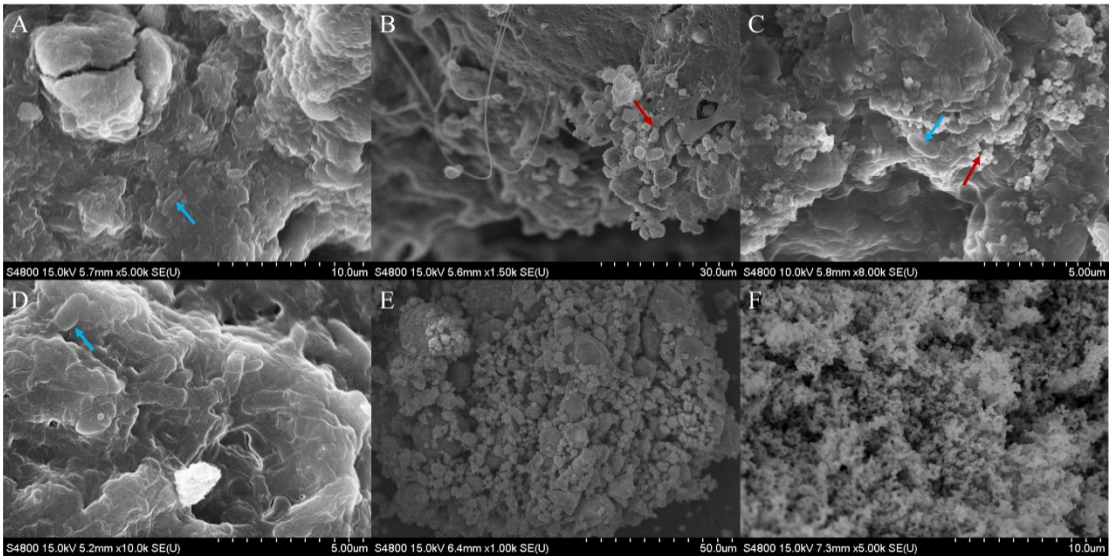

Figure S12. SEM images of granular sludges sampled from UASB reactors at the end of the experiment, (A) and (D) from black reactor R_1, (B) from TiO_2-added reactor (R_2), (C) from Fe_3O_4-added reactor (R_3), (E) pure TiO_2 nanoparticles, and (F) pure Fe_3O_4 nanoparticles. Blue arrows mark the bacteria, red arrows mark the nanoparticles.

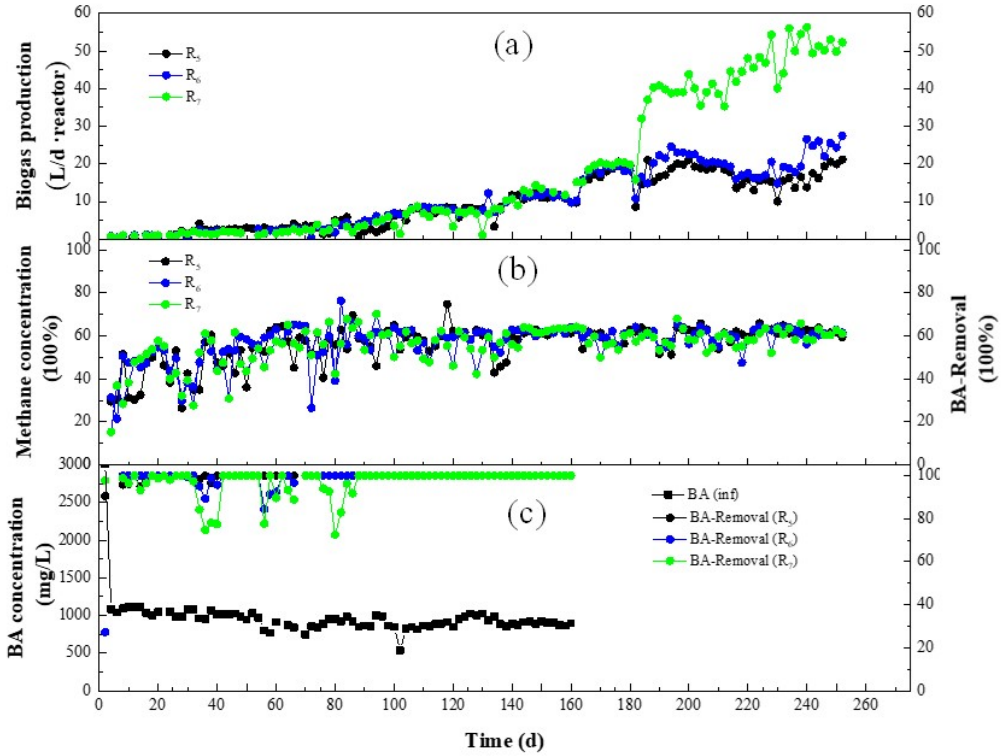

Figure S13. Variations of the biogas productions over operation days (a), methane concentrations (b), and degradation rates of BA in R_5 (blank), R_6 (TiO_2-added) and R_7 (Fe_3O_4-added).

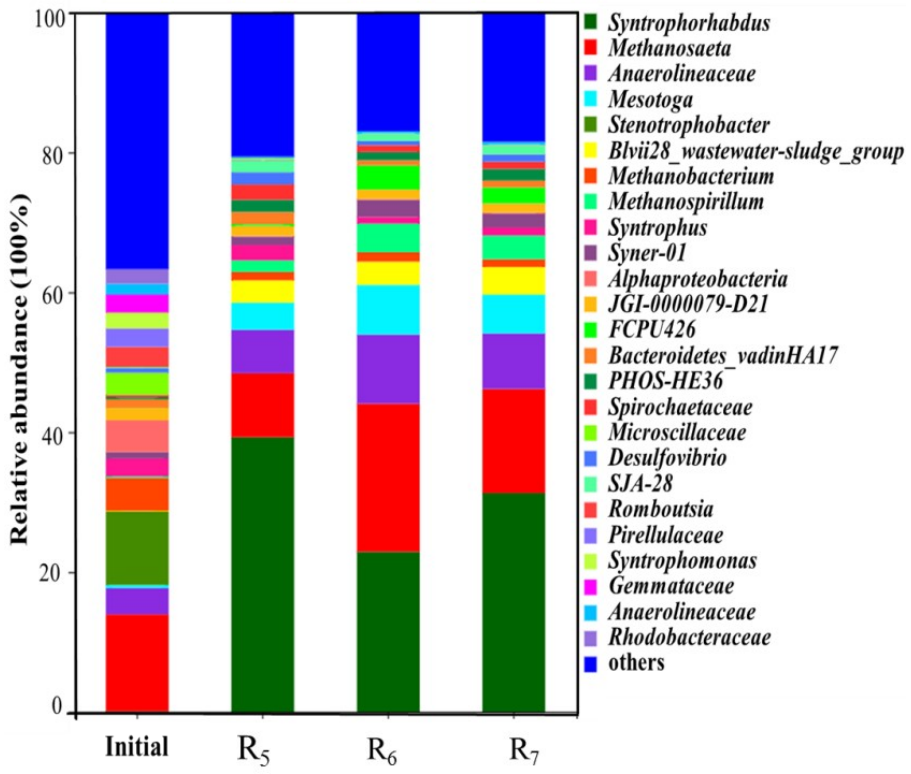

Figure S14. Community analysis of granular sludge samples at genus level in R_5 (blank), R_6 (TiO_2-added) and R_7 (Fe_3O_4-added).

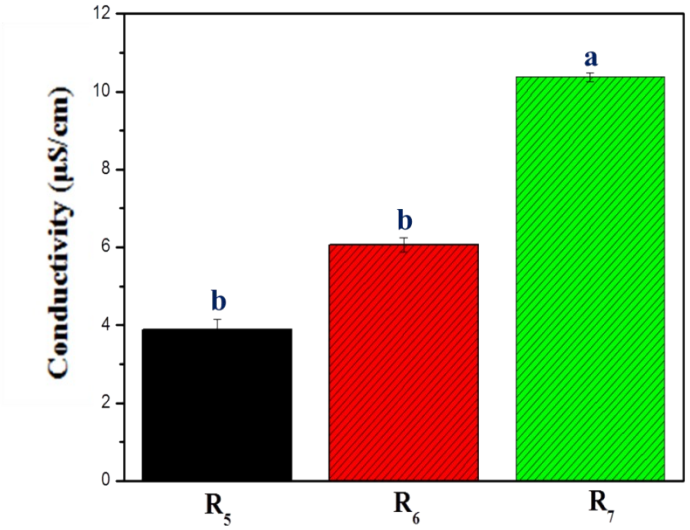

Figure 15. Conductance of granular sludges, R_5 for blank group, R_6 for TiO_2 supplemented group, R_7 for Fe_3O_4 supplemented group. Data of the different reactors marked with different case letters were significantly different at $p < 0.05$.

References

1 C.Q. Wang, L. Ye, J. Jin, H. Chen, X.Y. Xu, L. Zhu, Magnetite nanoparticles enhance the performance of a combined bioelectrode-UASB reactor for reductive transformation of 2,4-dichloronitrobenzene, *Sci. Rep.*, 2017, **7**, 10319.

2 G. Baek, H. Jung, J. Kim and C. Lee, A long-term study on the effect of magnetite supplementation in continuous anaerobic digestion of dairy effluent - Magnetic separation and recycling of magnetite, *Bioresource Technol.*, 2017, **241**, 830-840.

3 Y. Q. Lei, L. X. Wei, T. Y. Liu, Y. Y. Xiao, Y. Dang, D. Z. Sun, D. E. Holmes, Magnetite enhances anaerobic digestion and methanogenesis of fresh leachate from a municipal solid waste incineration plant, *Chem. Eng. J.* , 2018, **342**, 992-999.

4 R.C. Edgar, B.J. Haas, J.C. Clemente, C. Quince, R. Knight, UCHIME improves sensitivity and speed of chimera detection, *Bioinformatics*, 2011, **27**, 2194-2200.

5 Q. Wang, G.M. Garrity, J.M. Tiedje, J.R. Cole, Naive Bayesian classifier for rapid assignment of rRNA sequences into the new bacterial taxonomy, *Appl. Environ. Microbiol.*, 2007, **73**, 5261-5267.

6 S.S. Chen, A.E. Rotaru, P.M. Shrestha, N.S. Malvankar, F.H. Liu, W. Fan, K.P. Nevin, D.R. Lovley, Promoting Interspecies Electron Transfer with Biochar, *Sci. Rep.*, 2014, **4**, 5019.

7 Y. Lei, L. Wei, T. Liu, Y. Xiao, Y. Dang, D. Sun, D.E. Holmes, Magnetite enhances anaerobic digestion and methanogenesis of fresh leachate from a municipal solid waste incineration plant, *Chem. Eng. J.*, 2018, **348**, 992-999.